Modelling of the Meromictic Fjord Hunnbunn (Norway) with an Oxygen Depletion Model (OxyDep)

E.V. Yakushev, E.I. Debolskaya, I.S. Kuznetsov, and A. Staalstrøm

Abstract A biogeochemical model OxyDep coupled with three-dimensional hydrodynamic model GETM was used to simulate the hydrophysical and biogeochemical regimes of the meromictic Fjord Hunnbunn over the summer period. The main goal was to parameterize the oxygen depletion processes resulting in formation of suboxic and anoxic conditions in the water column. OxyDep considered five state variables: dissolved oxygen, inorganic nutrient, dissolved organic matter, particulate organic matter, and biota. This model parameterized the main processes responsible for the changing of the water column oxygen conditions – i.e. organic matter (OM) synthesis; OM decay due to oxic mineralization and denitrification; consumption of oxygen from sulphur and metals oxidation; and the processes at the boundaries (air–water exchange and the sediment–water exchange). Results of numerical experiments have reproduced the main features of the observed structure and have allowed to reveal the main components responsible for the formation of biogeochemical structure of the meromictic water objects. With the hydrodynamical model block used it was impossible to reproduce the presence of a permanent pycnocline. We suppose that special attention must be paid when using terrain following vertical coordinates (i.e. GETM) to avoid spurious vertical mixing. The results also showed that an application of simplified biogeochemical model blocks can be used as a useful tool for analysing and forecasting oxygen and nutrient regime changes.

E.V. Yakushev (✉) and A. Staalstrøm
Norwegian Institute for Water Research, Gaustadalleen 21, 0349 Oslo, Norway
e-mail: eya@niva.no

E.I. Debolskaya
Water Problems Institute of The Russian Academy of Science, Gubkina 3, 119991 Moscow, Russia

I.S. Kuznetsov
Leibniz Institute for Baltic Sea Research, Warnemünde, Seestrasse 15, 18119 Rostock, Germany

E.V. Yakushev (ed.), *Chemical Structure of Pelagic Redox Interfaces: Observation and Modeling*, Hdb Env Chem (2013) 22: 235–252, DOI 10.1007/698_2011_110,

Keywords Anoxia, Hydrogen sulphide, Hypoxia, Modelling, Oxygen depletion, Stratified basin

Contents

Abbreviations

BIO	Biota
DIN	Dissolved inorganic nitrogen (i.e. a sum of nitrate, nitrite, and ammonia)
DOM	Dissolved organic matter
GETM	General Estuarine Transport Model
NUT	Inorganic nutrient
OM	Organic matter
OXY	Dissolved oxygen
OxyDep	Oxygen Depletion biogeochemical model
POM	Particulate organic matter
PSU	Practical salinity units

1 Introduction

Oxygen depletion and anoxia formation are common features observed in many inland waters and coastal areas. These conditions arise, when transport rates of organic matter (OM) and oxygen into deeper layers do not balance and oxygen is used up during OM decomposition. The OM decomposition then continues via denitrification (consumption of oxidized forms of nitrogen: nitrate, NO_3 and nitrite, NO_2), and finally with reduction of sulphate (a major constituent in seawater). According to recent estimates [1], dead zones connected with low oxygen content have spread exponentially since the 1960s. Formation of oxygen-deficient, hypoxic, and anoxic conditions depend on the combined influence of eutrophication (amounts of nutrient loading) and intensity of mixing and water renewal.

The natural state of such complex systems with changeable redox conditions can be efficiently analyzed with mathematical models. The problem of an elaboration of a biogeochemical block for different redox conditions is connected with a necessity

of parameterizing switches between the processes dominating in oxic conditions (i.e. nitrification), hypoxic conditions (denitrification), and suboxic conditions (loss of oxygen for mineralization of reduced forms of sulphur and redox metals).

As mentioned in another chapter of this book [2], a threshold from oxic to hypoxic conditions is arbitrarily set at a bounding value of 2 mg O_2 L^{-1} (~63 μM O_2). Such thresholds can be connected with responses and vulnerability of pelagic and benthic animals, usually in the range of 1–4 mg O_2 L^{-1} [3]. The threshold between hypoxic and suboxic conditions (about 10–30 μM O_2 [4]) should reflect the oxygen level where oxygen becomes an auxiliary oxidant compared with nitrates and oxidized forms of metals.

The goal of this study was to elaborate a simplified biogeochemical model for the oxygen regime simulation and to apply it for a concrete object. This model should parameterize the changes in the biogeochemical processes in case of change of the oxygen concentrations from oxic to suboxic levels. We used a coupled Oxydep/GETM model to calculate the seasonal variability of the meromictic Fjord Hunnbunn.

2 Materials and Methods

2.1 Hunnbunn Hydrophysical and Hydrochemical Structure

At present, the Fjord Hunnbunn (Fig. 1) is a natural meromictic pool with the high concentrations of hydrogen sulphide in deep layers. Stratification of the lake is caused by a strong halocline. Wind and tidal waves arriving from the sea through the narrow channel Talbergsundet (length of 1.8 km) are mixed in the upper 2 m less saline layer, while the saline bottom layer remains unmixed. The maximum depth of the Fjord is about 11 m [5, 6].

Meanwhile, a history of the observations in the Hunnbunn reveal that the oxygen conditions there were much better in the past. Information from the past indicates that there were oysters in the nineteenth century [6]. An intensive eutrophication period and an absence of periodic dredging after the 1950s resulted in changes of the surface layer ecosystem: disappearance of the oysters, decline of seagrass beds, appearance of large amounts of green algae.

The present vertical hydrochemical structure of the Fjord Hunnbunn (Fig. 2) is typical for the coastal objects with anoxic conditions in the water column.

In 2009, the chemical structure of Hunnbunn was studied twice: in spring, 07.05.2009 and in late summer, 19.08.2009. We used a specially designed pump system for the redox-layers studies that allowed us to sample water with fine-scale resolution and prevented atmospheric oxygen from interfering with our results. The analytical determinations were made at the NIVA chemical laboratory according to the accredited national and international techniques [7]. During sampling, we used an AADI Oxygen Optode to measure the in situ oxygen concentrations.

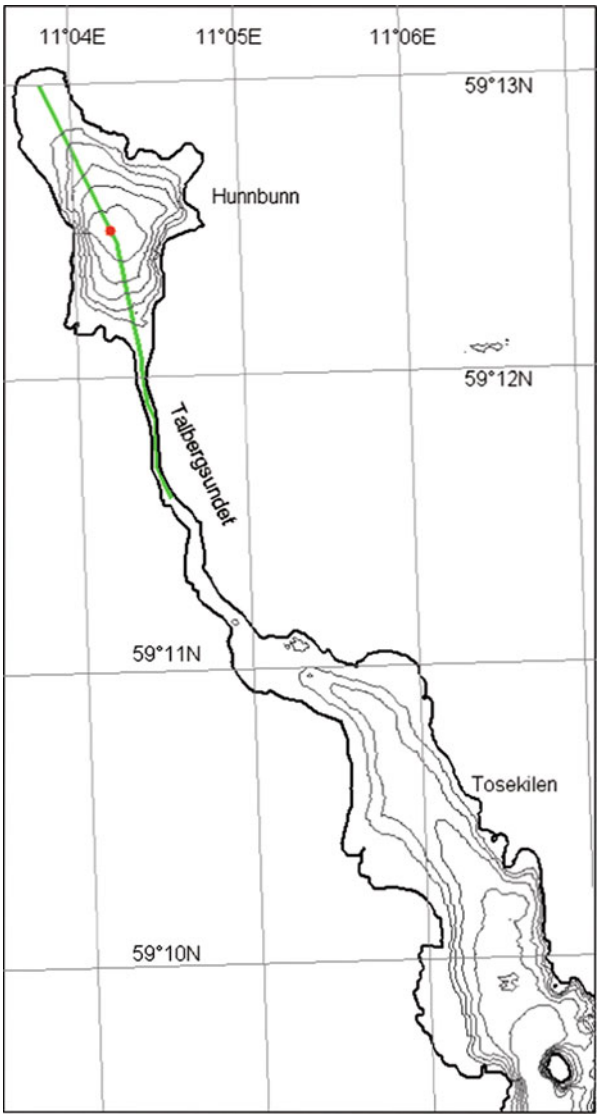

Fig. 1 A map of the Fjord Hunnbunn. Depth isolines are shown with 2-m interval. The position of hydro chemical data is marked with a red dot

The results of the studies performed in August 2009 are shown in Fig. 2. The vertical hydrochemical structure is typical for coastal objects with anoxic conditions in the water column. The concentration of dissolved inorganic nitrogen DIN (a sum of nitrate, nitrite, and ammonia) in the surface layer in May were high (5 μM), and concentrations of phosphate (0.06 μM) were low. Just below the oxygen maximum, at 4 m, the concentrations of phosphate increased to 6.5 μM, while concentrations of DIN decreased to 0.4 μM. There were no measurements in

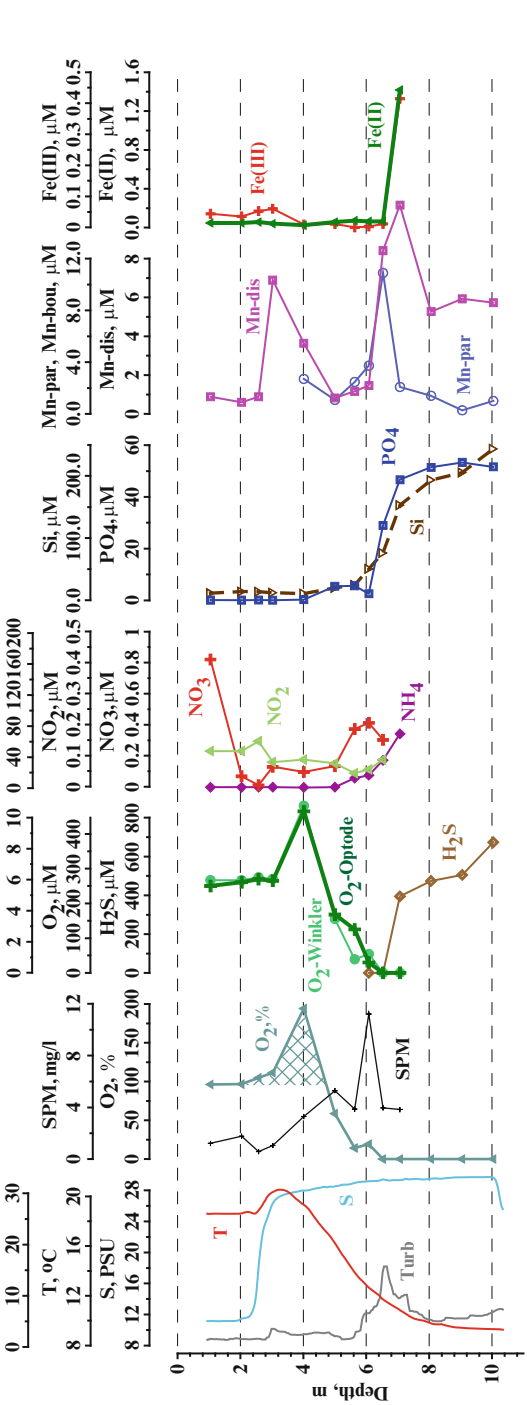

Fig. 2 Vertical hydrochemical structure of Hunnbunn 19.08.2009. *T* temperature, *S* salinity, *Turb* Turbidity, O_2% oxygen in percentages, *SPM* suspended particulate matter, *O2-Winkler* oxygen determined with Winkler technique, *O2-Optode* oxygen determined with AANDERAA Optode, H_2S hydrogen sulphide, NO_3 nitrate, NO_2 nitrite, NH_4 ammonium, PO_4 phosphate, *Si* silicate, *Mn-dis* dissolved manganese, *Mn-part* particulate manganese, *Fe(III)* dissolved trivalent iron, *Fe(II)* dissolved bivalent iron (from [5])

the vicinity of the oxygen maximum peak, but it is possible to assume that in May there were enough nutrients to support the high primary production.

In August, we made a fine resolution sampling for both oxygen and for nutrients. The oxygen concentration was slightly less than in May (10.7 ml/l in August), but the saturation value exceeded 194%, indicating very high primary production. In the vicinity of the oxygen maximum, we found 0.33 μM of phosphate, 1.2 μM DIN, and 10 μM of silicate. The vertical gradient of phosphate was more than 5 μM m^{-1} and DIN was 12 μM m^{-1}. Such large gradients ensure a permanent flux of nutrients from anoxic zone, sufficient to support the constant extremely high primary production throughout the year. The data received in August, 2009, revealed that below the depth of oxygen and nitrate depletion, reduced forms of sulphur (hydrogen sulphide), nitrogen (ammonia), manganese (Mn(II)), and iron (Fe(II)) were present. The concentrations of hydrogen sulphide increased in the bottom layer (10 m) to more than 600 μM (for a comparison, in the Black Sea the concentrations of hydrogen sulphide are 380 μM at the depth of 2,000 m). The concentrations of ammonia and phosphate in the Hunnbunn bottom layer are extraordinarily high and correspond to their concentrations in the pore water of the sediments from productive regions. All this indicates a very high level of OM concentrations in the Hunnbunn sediments and the bottom layer.

The concentrations of reduced forms of Mn and Fe are typical for the anoxic waters [8]. Mn does not accumulate in OM, and its distribution is determined by the flux from the sediments, if the water above is anoxic. That is why the observed maximum concentration of Mn(II) in Hunnbunn (12 μM) is comparable with that in the Black Sea (10–12 μM) and the Gotland Deep of the Baltic Sea (5–30 μM). Usually, Mn species are not observed in the oxic layer, because the oxidized heavy particles of Mn(IV) sink down just after their formation. The presence of significant concentrations of Mn and Fe species in the oxic zone points to an existence of their flux from the shore, that can also be observed in some other coastal regions.

The permanently observed redox-layer turbidity maximum in the Fjord Hunnbunn is a typical feature of anoxic systems. The nature of this turbid layer is not clear yet, but it is known that particulate forms of sulphur (element sulphur), manganese, iron, and bacteria can be found there. In case of the Fjord Hunnbunn, an additional large contribution to the turbidity can be made by photosynthetic purple bacteria, that can oxidize hydrogen sulphide using light. Usually, they are found in the upper part of the turbidity maximum and sometimes the turbidity maximum has two peaks as was observed in May 2009. The turbidity maximum in the Fjord Hunnbunn, might also be a "joint" maximum, where the redox-layer turbidity maximum combines with the phytoplankton maximum, typical for all the surface waters.

At present the OM produced in the Fjord Hunnbunn accelerates the depletion of oxygen and production of hydrogen sulphide, that lead to a positive feedback in a further increase in the flux of nutrients to the euphotic zone.

The anoxic layers of Fjords as Hunnbunn can be flushed with the a pulse of oxygen-rich cold water during the winter mixing either every year (Elefsis Bay in the Mediterranian Sea [9]) or every several years (Baerumsbassenget in the Oslo Fjord [10]) or every several decades (Fjord Framvaren). The probability of the

winter mixing depends on the topography, hydrophysical regime, and climate (weather conditions during the winter). The permanent pycnocline that exists in the Fjord Hunnbunn at the depth 2.5–3 m greatly hampers the flushing of the bottom layer.

2.2 GETM Application and Set Up

The model GETM (http://www.getm.eu) was used to simulate hydrodynamic and thermal regime of the Fjord, connected with the time-dependent changes in stratification and an influence of the tidal wave coming through the narrow channel. The density stratification changed in the Fjord not only due to meteorological factors, but with the seasonal fluctuations in salinity of water flowing through the channel [6]. The period of the tidal wave equaled to 12 h, the amplitude at the entrance to the lake was 0.5 m. The salinity at the entrance to the Fjord varied between 27 PSU in winter to 7 PSU during the spring flood.

These model simulations covered one year with a horizontal resolution of 50×50 m and 10 vertical layers. GETM is a terrain following model (sigma-coordinates model) and the vertical grid step changed from 20 cm to 1 m. The simulation is carried out on a grid with $90 \times 47 \times 10$ points. The time-step of calculations was 2 s.

The model was forced by the atmospheric forcing (seasonal changes in temperature and wind), and by providing information on temperature, salinity, and sea surface elevations at the lateral boundaries.

Freshwater discharge was not included in this simulation, because there are no significant fresh water flowing into Hunnbunn.

The general equation that is used for the coupled hydrodynamical–biogeochemical models is the following:

$$\frac{\partial C}{\partial t} + \nabla C\vec{V} - \nabla(K\nabla C) = R_C - \frac{\partial}{\partial z}(w_C C) \tag{1}$$

Where the first term reflects the changes with time, the second term reflects advective transport, and the third term reflects turbulent exchange. R_C is the biogeochemical sink/source terms for the considered variables, C is the concentration of a variable and w_C is the sinking rate of the particulate matter. We used GETM to calculate the velocities ($\vec{V}$) and the turbulent coefficient (K).

2.3 OxyDep Description

The idea behind OxyDep is to parameterize the changes of the biogeochemical processes in the water column and at the sediment/water boundary in case of

Table 1 State variables of the OxyDep

Variable	Meaning	Units
BIO	That is all the biota from bacteria to fish. BIO grows due to photosynthesis, loses inorganic matter due to respiration, and loses total (particulate and dissolved) organic matter due to metabolism, mortality, cannibalism, etc.	μM N
NUT	That is the oxidized forms of nutrients (i.e. NO_3 and NO_2 for N), that don't need additional oxygen for nitrification.	μM N
POM	That is all kinds of labile particulate organic matter (detritus).	μM N
DOM	That is all kinds of labile dissolved organic matter and reduced forms of inorganic nutrients (i.e. NH_4 and Urea for N).	μM N
OXY	Concentrations of dissolved oxygen.	μM O

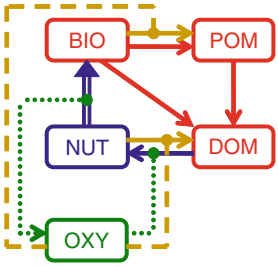

Fig. 3 Flow-chart of biogeochemical processes in the OxyDep

transition from oxic to suboxic conditions, and from suboxic to anoxic conditions in the simplest possible way. We aimed to receive a simple tool capable of being coupled to detailed 3D models (i.e. GETM [11], ROMS [12], HAMSOM/ECOSMO [19]) first of all for applications in shallow water, i.e. estuaries, inlets, and Fjords.

The amount of variables (Ci) and processes included in the parameterizations should depend on the different processes' time scales and the scales of concentrations [13]. In case of studying the behaviour of large concentration scale parameters (i.e. oxygen and nutrient, with characteristic concentrations of 10^1–10^2 μM) at relatively large time scale (seasonal) it is possible to merge the biological variables in one compartment (with characteristic concentrations less than 10^{-2}–10^{-1} μM) that was made here. List of the state variables (C_i) of the model is presented in the Table 1.

The flow-chart of biogeochemical processes considered in the OxyDep is shown in Fig. 3. Notations, values, units, and names of the model's parameters are given in Table 2. The biogeochemical changes of the considered variables, $R_{Ci,}$ were described with the following system of equations:

$$R_{BIO} = GrowthBIO - RespBIO - ExcrBIO - MortBIO$$
$$R_{POM} = -DissPOM + MortBIO - DecayPOM$$
$$R_{DOM} = DissPOM + ExcrBIO - DecayDOM$$
$$R_{NUT} = -GrowthBIO + RespBIO + DecayPOM + DecayDOM - DenitrOM$$
$$R_{OXY} = C_{OtoN}R_{NUT} + SMnOXY$$

Table 2 Notations, values, units, and names of parameters used in the model

Notation	Value	Units	Parameter
$GrowthBIO$		d^{-1}	Specific growth rate
$f_i(i)$		–	Photosynthesis dependence on irradiance
$f_\varphi(\varphi)$		–	Irradiance dependence on latitude
$f_t(t)$		–	Photosynthesis dependence on temperature
$f_n(NUT)$		–	Photosynthesis dependence on nutrient
K_{NB}	4.0	d^{-1}	Maximum specific growth rate
I_0	80.	W m^{-2}	Optimal Irradiance at the surface
k	0.10	m^{-1}	Extinction coefficient
I_{opt}	25.	W m^{-2}	Optimal irradiance
b_m	0.12	$°C^{-1}$	Coefficient for uptake rate dependence on t
c_m	1.4	–	Coefficient for uptake rate dependence on t
K_{NUT}	0.02	–	Half-saturation constant for uptake of NUT by BIO
K_{BN}	0.05	d^{-1}	Specific respiration rate
K_{BP}	0.01	d^{-1}	Specific rate of mortality in oxic conditions
K_{BD}	0.10	d^{-1}	Specific rate of excretion
K_{BP}^A	0.5	d^{-1}	Specific rate of mortality in anoxic conditions
K_{BP}^C	0.6	d^{-1}	Specific rate of additional mortality (cannibalism)
BIO_{Can}	1.	μM N	Threshold BIO value for cannibalism
K_{Can}	0.8	–	Coefficient for the cannibalism description
K_{PD}	0.10	d^{-1}	Specific rate of POM decomposition (autolis)
DecayDOM		d^{-1}	Mineralization of POM
K_{POM}	0.003	d^{-1}	Specific rate of POM oxic decay
K_{POM}^S	0.001	d^{-1}	Specific rate of POM denitrification
DecayDOM		d^{-1}	Mineralization of DOM
K_{DOM}	0.05	d^{-1}	Specific rate of DOM oxic decay
K_{DOM}^S	0.0005	d^{-1}	Specific rate of DOM denitrification
t_{da}	13.	–	Coefficient for dependence of decay on t
Bda	20.	–	Coefficient for dependence of decay on t
B_u	0.22	d^{-1} m^{-1}	Burial coefficient for lower boundary
NUT_{Den}	1.	μM N	Threshold NUT value for denitrification
C_{OtoN}	−8,625	–	O to N Redfield ratio (138/16)
$f_s(OXY)$		–	Function parameterizing a switches between oxic and suboxic processes
O_2^{bf}	20	μM O	Oxygen threshold concentration, in which the changes between suboxic and oxic processes occur
τ_L	100,000	s	Relaxation time
C_{L0}^O	0	μM O	Concentrations of OXY in the sediments in oxic conditions
C_{Li}^O	0	μM O	Concentrations of OXY in the sediments in suboxic conditions
C_{L0}^D	2	μM N	Concentrations of DOM in the sediments in oxic conditions
C_{Li}^D	5	μM N	Concentrations of DOM in the sediments in suboxic conditions
a_0	31.25	μM O,	Coefficient for the oxygen saturation calculations
a_1	14.603		Coefficient for the oxygen saturation calculations
a_2	0.4025	$°C^{-1}$	Coefficient for the oxygen saturation calculations
w_C	0.5	m d^{-1}	Sinking velocity

These biogeochemical sources where added to the general equation. These processes were parameterized as follows:

The specific growth rate of BIO,

$$GrowthBIO = K_{NB}\, f_t(t)\, f_i(i)\, f_n(NUT)BIO$$

is a function of temperature, light, and availability of nutrients with the maximum specific growth rate K_{NB}.

To describe the dependence of light in accordance to:

$$f_i(i) = f_\varphi(\varphi)\frac{i}{I_{opt}}\exp\left(1-\frac{i}{I_{opt}}\right).$$

we used the following parameters: light (i = $I_0 exp(-kh)$), incident light (I_0), optimal light (I_{opt}), extinction coefficient (k), depth (h), and variation of light with latitude and time:

$$f_\varphi(\varphi) = \cos\left(\varphi - \varphi_e \sin\left(2T/365.2\right)\right),$$

where T is time (days) and φ is latitude (degrees), $\varphi_e = 23.5$ is the ecliptic degree.

The following formula was chosen for dependence on temperature (t) with the coefficients b_m and c_m:

$$f_t(t) = \exp(b_m t - c_m).$$

A dependence with fast saturation of nutrient availability was used for NUT limitation description instead of traditional Michaelis–Menten formula:

$$f_n(NUT) = \frac{(NUT/BIO)^2}{(NUT/BIO)^2 + K_{NUT}^2},$$

where K_{NUT} is a "half saturation constant" for this dependence.

BIO respiration is described by specific rate of respiration K_{BN} as

$$RespBIO = K_{BN}BIO.$$

The excretion rate of *BIO* with specific rate of excretion K_{BD} was described as

$$ExcrBIO = K_{BD}BIO.$$

The natural mortality rate of BIO with specific rates of mortality K_{BP} in oxic and K_{BP}^A in anoxic conditions was described as:

$$\begin{aligned} MortBIO = {} & K_{BP}\mathrm{BIO} + f_S(\mathrm{OXY})K_{BP}^A\mathrm{BIO} \\ & + K_{BP}^C(0.5(1 - \tanh(BIO_{Can} - K_{Can}\mathrm{BIO})\mathrm{BIO}. \end{aligned}$$

The last term was added to parameterize an additional mortality due to "cannibalism", that starts when the BIO concentrations exceeds the threshold value BIO_{Can}.

We considered the formation of DOM from POM (autolysis) with a constant specific rate as:

$$DissPOM = K_{PD}POM.$$

The DOM decay took place due to oxic decay in oxic conditions (first term in the following equation) and denitrification in suboxic conditions (second term):

$$DecayDOM = K_{DOM}f_t^D(t)\mathrm{DOM} + K_{DOM}^S f_t^D(t) f_S(\mathrm{OXY}) f_N^D(\mathrm{NUT})\mathrm{DOM},$$

where $f_t^D(t)$ and $f_t^D(\mathrm{NUT})$ are dependences of decay on temperature and NUT.

The POM decay was parameterized as:

$$DecayPOM = K_{POM}f_t^D(t)\mathrm{POM} + K_{POM}^S f_t^D(t) f_S(\mathrm{OXY}) f_N^D(\mathrm{NUT})\mathrm{POM}.$$

The dependences of decay on temperature, $f_t^D(t)$, was parameterized as:

$$f_t^D(t) = B_{da}\frac{t^2}{t^2 + t_{da}^2},$$

where B_{da} and t_{da} are temperature control coefficients, and $f_t^D(\mathrm{NUT})$ is the dependences of decay on NUT (checking for availability of NO_3 and NO_2 necessary for denitrification).

$$f_N^D(\mathrm{NUT}) = 0.5(1 + \tanh(NUT - NUT_{Den})),$$

where NUT_{Den} is a threshold value.

The changes between the processes occurring in oxic and suboxic conditions were parameterized with soft switches based on hyperbolic tangents functions shown in Fig. 4:

$$f_O(\mathrm{OXY}) = 1 - 0.5\left(1 + \tanh\left(\mathrm{OXY} - {O_2}^{\mathrm{bf}}\right)\right)$$

and

$$f_S(\mathrm{OXY}) = 0.5\left(1 + \tanh\left(\mathrm{OXY} - {O_2}^{\mathrm{bf}}\right)\right),$$

where ${O_2}^{\mathrm{bf}}$ is a constant that defines the oxygen concentration, in which the changes occur.

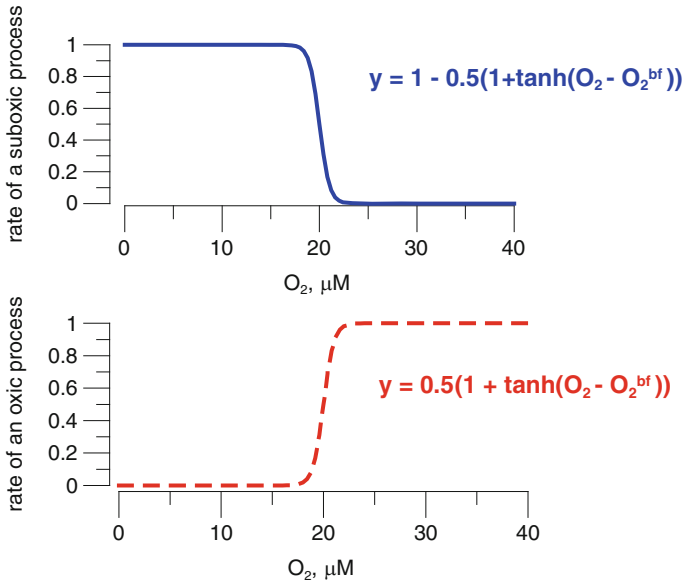

Fig. 4 Functions used as switches between oxic and suboxic processes (shown in Table 1.) assuming oxygen concentration $O_2^{bf} = 20$ μM as a threshold value

Changes in the OXY content were calculated with the Redfield ratio. Besides this, we parameterized an additional sink of oxygen for oxidation of reduced forms of sulphur and Mn. On the base of the estimates received in [14], we assumed for the oxygen deficient and suboxic conditions the consumption of oxygen for the mentioned purpose is similar to that for ammonia (that is a dominant part of DOM in OxyDep):

$$SMnOXY = f_S(\mathrm{OXY})K_{DOM}f_t^D(t)\mathrm{DOM}.$$

Changes in the NUT due to denitrification on particulate and dissolved organic were described as:

$$\begin{aligned} DenitrOM = {} & K_{POM}^S f_t^D(t) f_S(\mathrm{OXY}) f_N^D(\mathrm{NUT})\mathrm{POM} \\ & + K_{DOM}^S f_t^D(t) f_S(\mathrm{OXY}) f_N^D(\mathrm{NUT})\mathrm{DOM}. \end{aligned}$$

Loss of NUT for oxidation of the reduced forms of sulphur and metals was ignored.

Therefore, OxyDep parameterize the changes in the main biogeochemical processes connected with variations of oxygen concentrations between high normoxic to suboxic, with following oxygen depletion to 0.

Notations, values, units, and names of parameters used in the model are given in Table 2.

2.4 Sinking

The sinking parameterized as the last term of equation (1) was considered for BIO and POM with the same sinking velocity $w_{C.}$ (Table 2).

2.5 Boundary Conditions

In case of the upper boundary, the surface fluxes of the modelled chemical constituents were assumed to be zero, except for OXY. The O_2 surface flux is prescribed by:

$$Q_{O_2} = p_{vel}(Oxsat - OXY),$$

where p_{vel} is the wind coefficient, $Oxsat = a_0(a_1 + a_2t)$ is the concentration of oxygen saturation as a function of temperature t, according to [15].

Simulations were carried out based on a mean wind speed of 2 m s^{-1}.

Parameterization of the lower boundary conditions under changing redox conditions requires description of changes in intensity and even directions of fluxes of certain parameters.

For particulate organic matter (BIO, POM), we assumed the decrease of concentrations due to burial (modified on the base of an approach used in [16]):

$$Q_{C_i} = -B_u H_{vert} C_i,$$

where B_u is the burial rate. H_{vert} is the model's vertical resolution.

The changes of the bottom layer concentrations of DOM and NUT in oxic conditions, following the approach used in [17], we parameterized as:

$$Q_{C_i} = \tau_L^{-1}(C_{Li} - C_i).$$

The term on the right hand side describes a "relaxation" of C_i towards the constant C_{Li} in the sediment with the relaxation time scale τ_L. This term is used to ensure that the "observed" concentration in the sediment does not exceedingly diverge from simulated C_i which is strongly influenced by biogeochemical processes and by the horizontal advection.

When oxic conditions are present in the bottom water, the flux of oxygen nitrate into the sediments along with the absence of fluxes of H_2S, Mn(II), Fe(II) into the water should be observed.

In the case of suboxic conditions in the bottom water, there should be an increased flux of oxygen into the sediments. To reflect this we assumed for OXY:

$$Q_{C_i} = \tau_L^{-1}(C_{Li}^O - OXY) + f_s(OXY)\tau_L^{-1}(C_{L0}^O - OXY),$$

where C_{Li}^O and C_{L0}^O are concentrations of OXY in the sediments in oxic and suboxic conditions The same dependence was used for NUT, that should reflect the flux of nitrate into the sediments necessary to support denitrification there.

For DOM, we assumed the same dependence modified:

$$Q_{C_i} = \tau_L^{-1}(C_{Li}^D - DOM) + f_s(OXY)\tau_L^{-1}(C_{L0}^D - DOM),$$

where C_{Li}^D and C_{L0}^D are concentrations of DOM in the sediments in oxic and suboxic conditions, correspondingly, that allowed to parameterize a sudden increase of ammonia in case of depletion of oxygen at the water/sediment boundary. An additional term of oxygen sink *SMnOXY* allowed also to parameterize a flux from the sediment of reduced forms of sulphur, Mn, and Fe that occur in suboxic conditions [18].

At the open channel boundary that was positioned in 1.5 km from the Hunnbunn, we parameterized a uniform distributions of OXY (280 μM), NUT(0.5 μM), BIO (0.01 μM), DOM (0 μM), and POM (0 μM).

3 Results and Discussion

The results of modelling of the Fjord Hunnbunn structure along a transect from the channel mouth to the head of the Fjord (see Fig. 1 green line) in summer (a snapshot) is shown in Fig. 5.

According to the observation [6], the spring consolidation of the pycnocline and its subsequent dissolution from August is the most notable feature of the Hunnbunn hydrography. A goal of the hydrophysical block of the model was to reproduce a structure including a pycnocline that will be stable for a significant period of time necessary for a formation of anoxic layer.

Our model was able to reproduce the formation of pycnocline, but it was not stable and dissolved shortly after its formation. Numerical experiments with different vertical stretching of the model's layers (with decreased distance between the layers below the surface and increased above the bottom and visa versa) always demonstrated the dissolution of the pycnocline because of intense mixing along the slopes.

The calculated summer hydrophysical structure (Fig. 5) was characterized by a gradual decrease of temperature from about 15.3 °C at the surface to 15.0 °C over the bottom, while salinity increases from 14.0 PSU at the surface to 15.0 PSU at the bottom.

With this hydrophysical structure, the model allowed simulation of the main features of the vertical biogeochemical structure of a water body with the bottom anoxia. Using the BIO model compartment allowed parameterizing of processes of

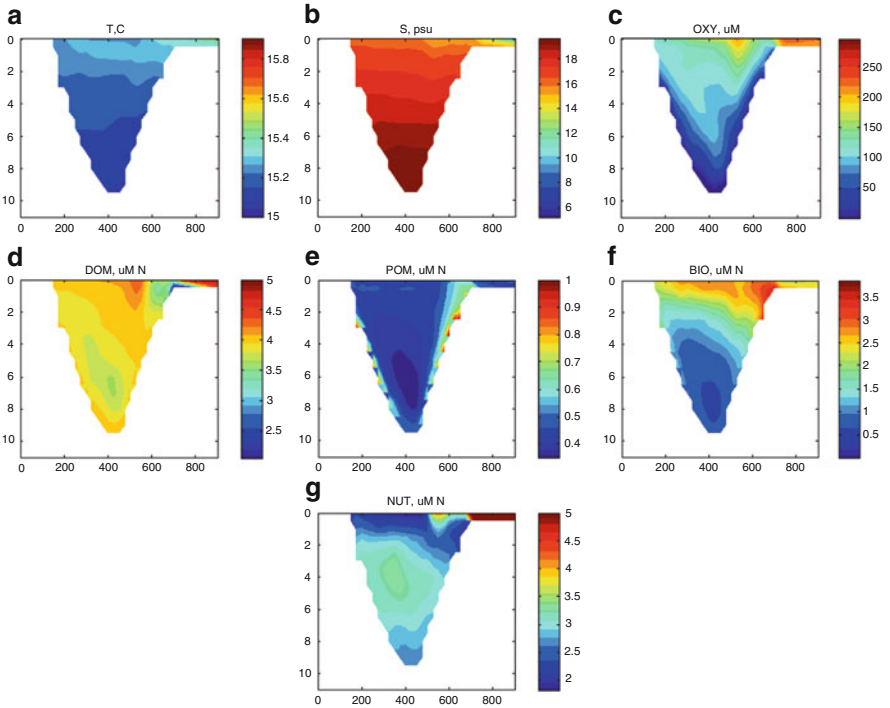

Fig. 5 The results of modelling of the Fjord Hunnbunn vertical structure at a transect from the channel mouth to the opposite coast in summer period for temperature, salinity, OXY, DOM, POM, BIO, and NUT

OM synthesis that resulted in the formation of high concentrations of DOM and POM. BIO had a maximum in the upper 0–2 m layer with concentrations 3.5 μM N (about 50 μg Chl-a L^{-1}) and decreased to 0 below 6 m depth. Concentrations of DOM varied from 5 μM in the euphotic later to approximately 3 μM at the 4–8 m depth, and increased to about 4–4.5 μM above the bottom. Maximum concentrations of POM were found directly at the bottom. The bottom layer near the channel mouth was enriched with BIO and organic matter compounds compared with the opposite flow slope.

Oxygen regime was determined by three factors: (1) production and consumption due to the synthesis and decay of OM, (2) exchange with the atmosphere, and (3) exchange at the bottom. OXY was characterized by maximum concentrations (200–280 μM) in the surface 0–2 m layer, where photosynthesis took place. Gas exchange secured high concentrations of oxygen in the surface layer. Below this layer oxygen was consumed by mineralization of OM (first of all in the dissolved form, DOM). The sinking of POM and BIO led to an enrichment of the bottom layer with OM. Here dissolved oxygen was quickly depleted for the mineralization of the water column POM and DOM, bottom POM and securing the flux from the sediments of DOM and reduced forms of sulphur and metals. This facilitated the

reproduction of anoxic conditions directly in the bottom and suboxic conditions in the 1–2 m layer above the bottom. The NUT (nitrate and nitrite) concentrations increased from about 2 μM N in the upper layer to 3.5–4 μM N at 4–6 m depth following by a decrease of concentrations above the bottom due to denitrification.

The model failed to simulate the formation of a thick 5 m anoxic zone in the modern Fjord Hunnbunn, but allowed reasonable reproduction of the characteristic features of a vertical biogeochemical structure with the bottom anoxia. The oxygen concentrations corresponding to suboxic conditions (less than 30 μM) were observed in the deep part of the modelled basin in a 2-m layer above the bottom. We hypothesise that a similar structure was in the Fjord Hunnbunn earlier when the oxygen regime was better [6].

The main reason for the difference between the simulated results and observed picture is that the hydrophysical block of the model failed to simulate the formation of a permanent developed pycnocline (halocline) that prevents the vertical exchange between the upper and low layers. We hypothesise that using a model with vertical sigma-coordinates (i.e. GETM) makes it very difficult to simulate a hydrophysical structure of shallow regions with pronounced pycnocline/halocline feature such as Fjord Hunnbunn and similar Fjords, lagoons and inlets. A necessity for the same amount of layers in all the grid points of the sigma-coordinates models results in significant changes of the physical vertical resolution (from about 1 m to 0.2 m in this model). At the slopes of the water body the enhanced exchange along the sigma-surfaces leads to an increased vertical transport of heat and salt that doesn't exist in nature.

4 Conclusions

We hypothesise that an application of a simplified biogeochemical model, OxyDep coupled with a 3D model (such as GETM, ROMS, HAMSOM) can be a useful tool for analysing and forecasting of oxygen and nutrient regime changes. In particular, it is possible to use the parameterized seasonal organic matter variability for studying of propagation of pollutants and carbonate system dynamics.

Special attention must be paid when using terrain following vertical coordinates to avoid spurious vertical mixing. The setup for the vertical coordinates in this particular model application needs to be tuned further to achieve more realistic vertical mixing. A z-coordinate model would probably conserve the vertical stratification like the one observed in Hunnbunn better.

Acknowledgements This research was supported by the Norwegian Institute for Water Research project 29083. The research leading to these results has received funding from the European Union's Seventh Framework Programme HYPOX under grant agreement n° 226213. We appreciate the help of colleagues for performing of the chemical analyses: S.V. Pakhomova, O.I. Podymov, and A.V.Kostyleva. We thank A.K. Sweetman for discussions and editing of the manuscript.

References

1. Diaz RJ, Rosenberg R (2008) Spreading dead zones and consequences for marine ecosystems. Science 321(5891):926–929
2. Yakushev EV (2011) RedOx layer model. In: Yakushev EV (ed.), Chemical Structure of Pelagic Redox Interfaces: Observation and Modeling, Hdb Env Chem (this volume)
3. Savchuk OP (2010) Large-scale dynamics of hypoxia in the Baltic Sea. In: Yakushev EV (ed.), Chemical Structure of Pelagic Redox Interfaces: Observation and Modeling, Hdb Env Chem DOI 10.1007/698_2010_53
4. Murray JW, Codispoti LA, Friederich GE (1995) The suboxic zone in the Black Sea. In: Huang CP, O'Melia R, Morgan JJ (eds) Aquatic chemistry: interfacial and interspecies processes. Adv Chem Ser 244. American Chemical Society, Washington DC, pp 157–176
5. Staalstrøm A, Bjerkeng B, Yakushev E, Christie H (2009) Water exchange and water quality in Hunnbunn – evaluation of dredging in the Thalbergsund with regard to improved water quality. NIVA report no. 5874–2009, p 53
6. Ström TE, Klaveness D (2003) Hunnebotn: a seawater basin transformed by natural and antohropogenic processes. Estuar Coast Shelf Sci 56(5–6):1177–1185
7. Grashoff K, Kremling K, Ehrhard M (1999) Methods of seawater analysis, 3rd completely revised and extended edition. Wiley–VCH, Weinheim
8. Pakhomova SV, Yakushev EV (2011) Manganese and iron at the redox interfaces in the Black Sea, the Baltic Sea, and the Oslo Fjord. In: Yakushev EV (ed.), Chemical Structure of Pelagic Redox Interfaces: Observation and Modeling, Hdb Env Chem DOI 10.1007/698_2011_98
9. Pavlidou A, Kontoyiannis H, Anagnostou Ch, Siokou–Frangou I, Pagou K, Krasakopoulou E, Assimakopoulou G, Zervoudaki S, Zeri K, Chatzianestis J, Psyllidou-Giouranovits R (2010) Biogeochemical Characteristics in the Elefsis Bay (Aegean Sea, Eastern Mediterranean) in relation to anoxia and climate changes. In: Yakushev EV (ed.), Chemical Structure of Pelagic Redox Interfaces: Observation and Modeling, Hdb Env Chem DOI 10.1007/698_2010_55
10. Berge JA, Amundsen R, Bjerkeng B, Bjerknes E, Espeland SH et al (2010) Overvåking av forurensningssituasjonen i Indre OsloFjord 2009. NIVA report no. 5985–2010, p 145
11. Stips A, Bolding K, Pohlman T, Burchard H (2004) Simulating the temporal and spatial dynamics of the North Sea using the new model GETM (General Estuarine Transport Model). Ocean Dyn 54:266–283
12. Shchepetkin AF, McWilliams JC (2005) The region ocean model system (ROMS): a split-explicit, free-surface, topography-following-coordinate oceanic model. Ocean Modell 9:347–404
13. Yakushev EV (2002) On parameterization of biogeochemical processes in modelling objects at different time scales. Electronic Journal Studies in Russia (Issledovano v Rossii) 141:1587–1594. http://zhurnal.ape.relarn.ru/articles/2002/141.pdf (in Russian)
14. Yakushev EV, Pollehne F, Jost G, Umlauf L, Kuznetsov I, Schneider B (2007) Analysis of the water column oxic/anoxic interface in the Black and Baltic seas with a Redox-Layer Model. Mar Chem 107:388–410
15. Neumann T, Fennel W, Kremp C (2002) Experimental simulations with an ecosystem model of the Baltic Sea: a nutrient load reduction experiment. Global Biogeochem Cycles 16(3)
16. Savchuk OP, Wulff F (2009) Long-term modelling of large-scale nutrient cycles in the entire Baltic Sea. Hydrobiologia 629:209–224
17. Yakushev EV, Kuznetsov IS, Podymov OI, Burchard H, Neumann T, Pollehne F (2011) Modeling of influence of oxygenated inflows on biogeochemical structure of the Gotland Sea, central Baltic Sea: changes in distribution of manganese. Comput Geosci 37:398–409
18. Skei J, Melsom S (1982) Seasonal and vertical variations in the chemical composition of suspended matter in an oxygen deficient Fjord. Estuar Coast Shelf Sci 14:61–78
19. Schrum C, Janssen F, Hubner U (2000) Recent climate modelling for North Sea and Baltic Sea. Part A: model description and validation. – Berichte des Zentrums für Meeres- und Klimaforschung, Universität Hamburg, p 37